CHARACTERIZATION OF THE REGIONS OF CONVERGENCE OF CMA ADAPTED BLIND FRACTIONALLY SPACED EQUALIZER

Wonzoo Chung and C. Richard Johnson Jr.**

School of Elec. Engineering
Cornell University
Ithaca, NY 14853

ABSTRACT

The constant modulus algorithm (CMA) is an effective and popular scheme for blind adaptive equalization. Delineation of the regions of convergence of this multimodal algorithm has remained as an unresolved problem in spite of its significance with regard to CMA initialization strategies. In this paper we present a qualitative analysis of convergence regions of the fractionally spaced CMA (FS-CMA) equalizer based on a new geometrical understanding of the constant modulus cost function. We characterize the location and volume of the convergence regions of local minima, and associate the volume of the convergence regions with their MSE performance. The convergence regions of the local minima with low noise gain expand near the origin, while those of the local minima with high noise gain shrink. This explains partly the robustness of FS-CMA and the MSE optimization achieved by the widely used center spike initialization with constrained magnitude.

1. INTRODUCTION

Adaptive equalization based on the constant modulus (CM) criterion, which exploits fourth order source statistics, is perhaps the best well known practical blind adaptive equalizer. The fractionally spaced equalizer adapted to descend the gradient of the CM criterion (FSE-CM) has been widely used and studied intensively [4]. Recent study of the mean squared error (MSE) performance of CM cost minimization applied to a fractionally spaced receiver has emphasized proper initialization of FSE-CM equalizer [6]. Since the knowledge of convergence regions is critical for initialization strategies, a theoretical description of convergence regions of local minima is desired.

We approach this problem with two novel "tricks". First, we decompose the FSE-CM cost function into a radial component and a spherical component, which correspond to noise gain and inter-symbol-interference (ISI) respectively. This provides a geometric understanding of FSE-CM and an immediate derivation of a closed-form expression of convergence regions in the system space. Second, we apply the system space result to the equalizer space of an arbitrary channel in a qualitative way. Just as with any (stochastic) gradient descent based adaptive equalizer, the FSE-CM cost function induces a gradient dynamic system on the equalizer space. Our analysis is focused on the dynamic system instead of the cost function. The dynamic system in the equalizer space of the given channel is represented by a linear coordinate transformed system (via the channel convolution matrix) from that of the system space. The convergence regions of the equalizer space of the FSE-CM for an arbitrary channel are result from this transformation, which performs rotation and dilation (determined by the singular decomposition of the channel convolution matrix).

The study on the effect of dilation reveals our main result on the convergence regions of FSE-CM: The convergence regions have a "exponential hypercone" structure and, hence, the convergence regions of small noise gain minima are (exponentially) expanded and those of large noise gains are shrunk (exponentially) near the origin (vice versa for far from the origin). The approximation we then use is motivated by an observed result that the spherical deformation of regions of convergence is ignorable in comparison to the radial (exponential) deformation. Thus, we use radial behavior alone to approximate regions of convergence. Although we assume a noise free model throughout our analysis, this trend of convergence regions is still valid for the moderate noise case, since below a certain SNR threshold noise simply causes smoothing effects on the FSE-CM error surface [2]. This result helps explain the asymptotic mean square error (MSE) optimization capabilities of a single spike initialization with constrained magnitude of FSE-CM.

2. SYSTEM MODEL

In Figure 1, We consider a fractionally spaced linear equalization of a time invariant linear channel model c in the ab-

*Supported by NSF Grants MIP-9509011 and ECS-9528363 and Applied Signal Technology.

0-7803-5148-7/98/$10.00©1998 IEEE

sence of noise.

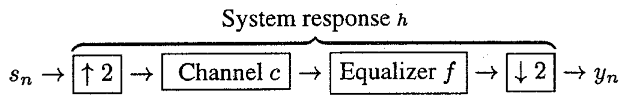

Figure 1 System Model

We utilize the so called perfect equalization assumptions [4] so that the equalizer parameter vector f is determined by the channel convolution matrix and overall system response h [4]

$$f = C^{-1}h. \tag{1}$$

Let H be the space of all system responses (*system space*) and F be the space of equalizers (*equalizer space*). Eq (1) induces an isomorphism between two vector spaces

$$C : H \cong F \tag{2}$$

In the next section we develop a full description on the convergence regions of the FS-CMA in the system space, and in section 4, we turn to the equalizer space.

3. REGIONS OF CONVERGENCE IN THE SYSTEM SPACE

3.1. Decomposition of FSE-CM cost function into Radial and Spherical terms

Fractionally spaced blind equalization using Constant Modulus Algorithm (FSE-CM) provides an adaptive algorithm for finding the equalizer minimizing following cost function

$$J(f) = E\left\{(|y(n)|^2 - \gamma)^2\right\} \tag{3}$$

with the update equation

$$f\text{new} = f - \mu \frac{\partial}{\partial f} J(f) \tag{4}$$

where $\gamma := m_4/m_2$, the ratio of the fourth moment (m_4) and the second moment (m_2) of the source, is called the dispersion constant. The goal of blind equalization in the absence of noise is to obtain *pure delays* ($[0 \cdots 1 \cdots 0]$) in H-space from the statistical information of the source. To quantify this objective, we define a measure of inter symbol interference (ISI) in H-space.

Definition 1 For any vector $h = [h_0 \cdots h_{N\text{-}1}]^T \in H$, *the inherent ISI of* h, I_h, is a real valued function on H defined by;

$$I_h := \sum_{i \neq j}^{N\text{-}1} |h_i|^2 |h_j|^2, \tag{5}$$

which is nonnegative definite.

Observe that $I_h \geq 0$ and $I_h = 0$ if and only if h is a pure delay.

Lemma 1 In the absence of channel noise, the FSE-CM cost function on the system space H, denoted by J_H, for a ciculary symmetric source (such as QAM) can be expressed [2] as

$$4J_H(h) = m_4(||h||^2 - 1)^2 + \gamma^2 - m_4 + \eta_s I_h, \tag{6}$$

where $||\cdot||$ is the ℓ_2-norm and η_s is defined as the kurtosis deviation of the source from the Gaussian kurtosis κ_w (with normalized kurtosis $\kappa_s := m_4/m_2^2$)

$$\eta_s := \kappa_w m_2^2 - m_4 = m_2^2(\kappa_w - \kappa_s)$$

Henceforth, we will assume a BPSK source and a real channel. The cost function is simplified to

$$4J_H(h) = \underbrace{(||h||^2 - 1)^2}_{\text{Radial term}} + \underbrace{2I_h}_{\text{Spherical term}} \tag{7}$$

Figure 2 illustrates an example of this decomposition for 2 dimensional case.

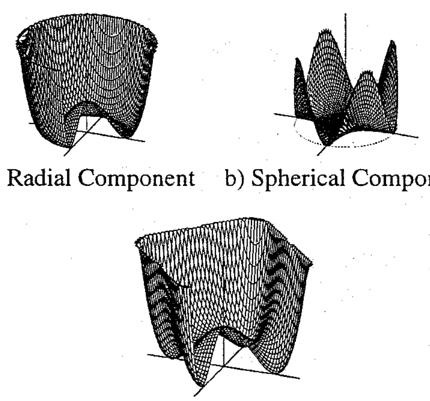

a) Radial Component b) Spherical Component

c) FSE-CM cost function

Figure 2 Decomposition of FSE-CM cost function

3.2. Regions of Convergence in the System Space

Consider the gradient system on the system space defined by the FSE-CM cost function

$$\nabla_h^H = -\frac{\partial}{\partial h} J_H(h). \tag{8}$$

The simplicity of the radial component, $(||h||^2 - 1)^2$, results in an important property of this vector field that local minima and saddle points under a FSE-CM gradient system are mostly characterized by the spherical term, more precisely, the spherical term restricted to the unit sphere $I_h|_{S^{N\text{-}1}}$. The local minima consist of pure delays [?] and the regions of convergence are obtained by solving $\frac{\partial}{\partial h} I_h|_{S^{N\text{-}1}}$, which can be associated with a set of hyperelipsoids in a geometrical representation.

Theorem 1 (Regions of Convergence on H) Let $\mathcal{R}(d_i)$ denote the regions of convergence of a local minima of FSE-CM, $d_i = [0, .., 0, 1(i\text{-th place}), 0...0]$. Then $\mathcal{R}(d_i)$ is a hypercone

$$\mathcal{R}(d_i) = \{h \in H \mid h_i > 0, \quad |h_i| > |h_k| \text{ for all } k \neq i\}, \quad \text{and } \mathcal{R}(-d_i) = -\mathcal{R}(d_i).$$

illustrated in Figure 3.

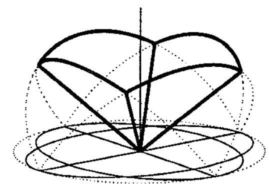

Figure 3 Regions of convergence in the system space

3.3. Simplified Vector Field Model for FSE-CM on the system space

Now we propose a simplified vector field model which extends the idea of decomposing FSE-CM into spherical and radial terms. FSE-CM has a unique radial minima in every direction $\hat{h} \in S^{N\text{-}1}$ which is given by

$$r(\hat{h}) = \sqrt{\frac{1}{1 + \eta_s I_{\hat{h}}}} \tag{9}$$

We define the set of radial minima $\left\{r(\hat{h})\hat{h} \mid \hat{h} \in S^{N\text{-}1}\right\}$ as the *radial minima surface* Φ [2, 5]. We can interpret the role of the radial term of FSE-CM roughly as bringing the parameter h onto Φ. The final stage of adaptation is often motion "along" ϕ. Since Φ is bounded by $1/\sqrt{1+\eta_s} < r(\hat{h}) \leq 1$, we approximate Φ with $S^{N\text{-}1}$. The proposed model is

$$\widetilde{\nabla}_h^H = \begin{cases} \nabla^\Phi & \text{for } \|h\| = 1 \\ -h & \text{for } \|h\| < 1 \\ h & \text{for } \|h\| > 1 \end{cases} \tag{10}$$

where ∇^Φ denotes the vector field on Φ derived from the cost function $I_h|_{S^{N\text{-}1}}$. Notice that $\widetilde{\nabla}_h^H$ is not itself a vector field. Figure 4 provides a comparison of a) ∇^Φ and b) $\widetilde{\nabla}_h^H$.

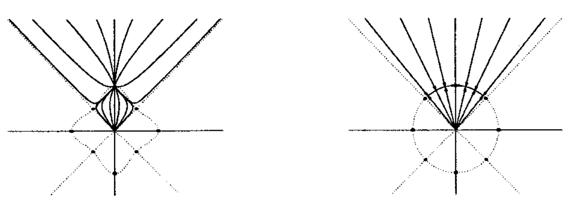

a) Trajectories of FS-CMA b) Trajectories of simplified model

Figure 4 Trajectories of FS-CMA and simplified model

4. REGIONS OF CONVERGENCE OF FS-CMA

4.1. The Relation between System Space Vector Field and Equalizer Space Vector Field

With C a channel convolution matrix of a $T/2$-spaced channel c, the relation between the vector field on the system space and the FSE-CM vector field on the equalizer space ∇_f^F is obtained from the relation $h = Cf$

$$\nabla_f^F = -\frac{\partial}{\partial f} J_H = -C^T \frac{\partial}{\partial h} J_H = C^T \nabla_{Cf}^H \tag{11}$$

From (11), we conclude every stationary point on the equalizer space is a $C^{\text{-}1}$-transformed stationary point on the system space. Therefore, the local minima of FSE-CM in equalizer space, denoted by f_i, are $\{\pm C^{\text{-}1} d_i \mid i = 0, .., N\text{-}1\}$. Notice that the norms of the local minima $\|f_i\|$ are distributed corresponding to the eigenvalues of $C^{\text{-}1}$.

In contrast to the stationary points, the regions of convergence of g_i, denoted by $\mathcal{R}(g_i)$, cannot be obtained from simple linear transformation, since the cost function is *nonlinear*. Therefore, we investigate the effects of a linear transformed vector field on the convergence regions.

Let $C = U\Lambda V^T$ be the singular decomposition of C (U, V are unitary matrix and $\Lambda = \text{diag}(\lambda_0, ..., \lambda_{N\text{-}1})$ with $\lambda_0 >, ..., > \lambda_{N\text{-}1} > 0$). The vector field ∇^F is rewritten as

$$\nabla_f^F = V\Lambda^T U^T \nabla_{U\Lambda V^T f}^H \tag{12}$$

Let $g_i = C^{\text{-}1} d_k$ be a local minimum on F under ∇^F. Then the region of convergence of g_i, $\mathcal{R}(g_i)$, is obtained from $\mathcal{R}(d_k)$ through the following process, which will be described in the following subsections.

1. "Rotate" $\mathcal{R}(Cg_i)$ under ∇^H by the unitary matrix U^T
2. "Dilate" $U^T(\mathcal{R}(Cg_i))$ by diagonal matrix Λ
3. "Rotate" again the stretched region of convergence, say $\mathcal{S}$, by the unitary matrix V

The chart below summarizes this process.

	Vector Field		Local minima		R.O.C.
On H :	∇^H	$\cdots$	$U\Lambda V^T g_i$	$\cdots$	$\mathcal{R}(Cf)$
	$\downarrow U^T$		$\downarrow U^T$		$\downarrow U^T$
	$U^T\nabla^H$	$\cdots$	$\Lambda V^T g_i$	$\cdots$	$U^T(\mathcal{R}(Cf))$
	$\downarrow \Lambda$		$\downarrow \Lambda^{\text{-}1}$		$\downarrow \Lambda$
	$\Lambda U^T \nabla^H$	$\cdots$	$V^T g_i$	$\cdots$	$\mathcal{S}$
	$\downarrow V$		$\downarrow V$		$\downarrow V$
On F :	$V\Lambda U^T \nabla^H$	$\cdots$	g_i	$\cdots$	$V(\mathcal{S})$

Example 1 Consider a $T/2$-spaced channel $c = [0.11,\ 0.8779,\ 0.3762,\ 0.2751]$. Then

$$C = \begin{bmatrix} 0.8779 & 0.11 \\ 0.2751 & 0.3762 \end{bmatrix} = \begin{bmatrix} \cos(\pi/8) & -\sin(\pi/8) \\ \sin(\pi/8) & \cos(\pi/8) \end{bmatrix} \begin{bmatrix} 0.9487 & 0 \\ 0 & 0.3162 \end{bmatrix} \begin{bmatrix} \cos(\pi/12) & -\sin(\pi/12) \\ \sin(\pi/12) & \cos(\pi/12) \end{bmatrix}$$

and the process above unfolds as shown in Figure 5.

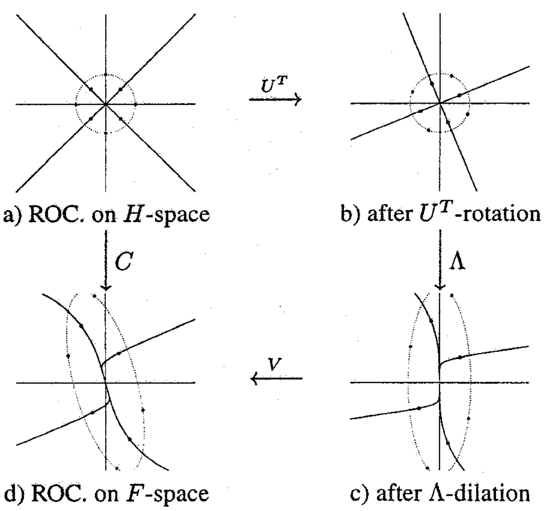

Figure 5 Regions of convergence of FSE-CM: Equalizer space through System space

In following subsections, each of the steps in Figure 5 will be described in detail.

4.2. Regions of Convergence of FSE-CM - Rotation

Lemma 2 (Rotation) Let ∇ be a given vector field on F and U be an unitary matrix. Denote ∇' as a vector field on F induced by U in the following way

$$\nabla'_f = U^T \nabla_{Uf}$$

Then, for a local minima f under ∇, $U^{-1}f$ is a local minima under ∇'. Denote the regions of convergence f as $\mathcal{R}(f)$ and that of $U^{-1}f$ under ∇' as $\mathcal{R}(U^{-1}f)$. It holds that

$$\mathcal{R}(U^{-1}f) = U^{-1}(\mathcal{R}(f))$$

4.3. Regions of Convergence of FSE-CM - Dilation

Unfortunately, the "dilation" part does not allow any closed form expression. We are limited to sketching a general trend by using an approximate model.

Let $\widetilde{\nabla}^H$ be the vector field model of FSE-CM on the system space defined in section 3.3. Let ∇' be a U-transformed vector field of $\widetilde{\nabla}^H$ (Lemma 2). Let $\{\mathcal{R}_i\}$ denote the regions of convergence under ∇' and $\{\mathcal{BR}_i\}$ denote those on Φ. By Lemma 2, $\{\mathcal{R}_i\}$ are rotated hyper-cones and $\{\mathcal{BR}_i\}$ equally divide Φ. We assume the rotation U is not so severe that $\mathcal{R}_i \subset \{F = UH \mid f_i > 0\}$ for each i.

Let $\Lambda = \mathrm{diag}(\lambda_0, \cdots, \lambda_{N\text{-}1})$ be a diagonal matrix with $\lambda_0 > \cdots > \lambda_{N\text{-}1} > 0$ and ∇ denote the Λ-transformed vector field model from ∇'. Since $\Lambda^T \nabla'_{\Lambda f} = \pm\Lambda^2 f$ for $f \notin \Lambda^{-1}\Phi$,

$$\nabla_f = \begin{cases} \nabla^{\Lambda^{-1}\Phi} & \text{for } f \in \Lambda^{-1}\Phi \\ -\Lambda^2 f & \text{for } \|\Lambda f\| < 1 \\ \Lambda^2 f & \text{for } \|\Lambda f\| < 1 \end{cases} \tag{13}$$

where $\nabla^{\Lambda^{-1}\Phi}$ denotes the vector field on $\Lambda^{-1}\Phi$ induced via Λ^{-1} from the ∇ on Φ. Under this model regions of convergence are determined by the spherical term $\nabla^{\Lambda^{-1}\Phi}$:

Let s_i be the local minima under ∇ and $\mathcal{S}_i$ be the convergence region of s_i, and $\mathcal{BS}_i$ be that of s_i on $\Lambda^{-1}\Phi$. Then the convergence region $\mathcal{S}_i$ has the following form from (13)

$$\mathcal{S}_i = \left\{ e^{t\Lambda^2} b \mid b \in \mathcal{BS}_i,\ t \in (-\infty, \infty) \right\}, \tag{14}$$

Since every trajectory is an exponential curve and they meet all at the origin, we label this an *exponential hyper-cone*.

Therefore, it is important to delineate $\mathcal{BS}_i \subset \Lambda^{-1}\Phi$, which is transformed by Λ^{-1} from $\mathcal{BR}_i \subset \Phi$. From the view of differential manifolds [1], the effect of Λ^{-1} on Φ under ∇ is characterized by the effect of Λ_i^{-1} on the $\pi_i\Phi$ under $\pi_i(\nabla)$ for $i = 0, ..., N\text{-}1$, where $\Lambda_i = \mathrm{diag}(\lambda_0, ..., \lambda_{i-1}, \lambda_{i+1}, ..., \lambda_{N\text{-}1})$ and π_i is a projection map ($\pi_i(x) = (x_0, ..., x_{i-1}, x_{i+1}, ..., x_{N\text{-}1})$). Let $x \in \pi_i(\Phi)$ and $y = \Lambda_i^{-1}x \in \Lambda_i^{-1}\pi_i\Phi$. Then, for a small step size μ, the trajectory of y under $\pi_i\nabla$ is generated by

$$y_{\text{new}} = \Lambda_i^{-1}(x + \mu\Lambda_i^2\pi_i\nabla_x)$$

The Λ_i^2 term introduces non-linear deformation, and thus $\mathcal{BS}_i$ does not agree with $\Lambda^{-1}\mathcal{BR}_i$ in general. However, the deformation does not cause significant difference between volumes of $\mathcal{BS}_i$ and $\Lambda^{-1}\mathcal{BR}_i$, though it causes a "convexing" effect on the shape as Example 2 shows. Hence, we approximate $\mathcal{BS}_i$ with $\Lambda^{-1}\mathcal{BR}_i$ by ignoring this less significant deformation.

Example 2 Let

$$U = \begin{bmatrix} \cos(\pi/8) & -\sin(\pi/8) & 0 \\ \sin(\pi/8) & \cos(\pi/8) & 0 \\ 0 & 0 & 1 \end{bmatrix}, \quad \Lambda = \begin{bmatrix} \lambda & 0 & 0 \\ 0 & 1 & 0 \\ 0 & 0 & 1 \end{bmatrix}$$

We consider the nonlinear deformation due to $\Lambda_2 = \mathrm{diag}(\lambda, 0)$. When $\lambda = 1$, $\pi_2(\mathcal{BR}_2)$ is a rotated projection of the convergence region in Figure 3 in Section 3.2 (Figure 6 a)). As λ increases the non-linear deformation starts (Figure 6 b)). In the asymptotic case, when $\lambda = \infty$, we have a polygon shape of which vertices consist of local minima and maxima (Figure 6 c)).

Convergence region of $(0, 0, 1)$

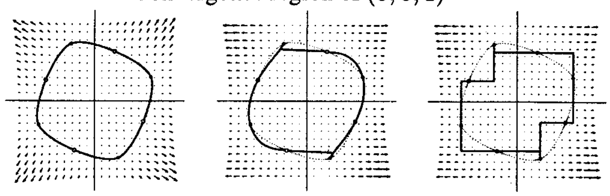

a) λ=1 b) $\lambda = 50$ c) $\lambda = \infty$

Figure 6 Deformation of Convergence on Φ by various λ

4.4. Noise gain and Regions of Convergence

We are interested in the volume of $\mathcal{S}_i$ near the origin. Let $\mathcal{DS}_i^\alpha$ be the convergence region of s_i on an α-radius sphere $\alpha S^{N\text{-}1}$ of F, i.e.,

$$\begin{aligned} \mathcal{DS}_i^\alpha &:= \mathcal{S}_i \cap \alpha S^{N\text{-}1} \qquad (15)\\ &\approx \alpha S^{N\text{-}1} \cap \left\{ e^{t\Lambda^2} b \mid b \in \Lambda^{\text{-}1}\mathcal{BR}_i,\ t \in (-\infty, \infty) \right\}. \end{aligned}$$

First we consider the projections of $\Lambda^{\text{-}1}\mathcal{BR}_i$ on $\alpha S^{N\text{-}1}$ via straight rays

$$\overline{\mathcal{DS}_i^\alpha} := \alpha S^{N\text{-}1} \cap \left\{ e^{tI} b \mid b \in \Lambda^{\text{-}1}\mathcal{BR}_i,\ t \in (-\infty, \infty) \right\} \quad (16)$$

Then, for $\lambda_i > \lambda_j$, Vol $\overline{\mathcal{DS}_i^\alpha}$ > Vol $\overline{\mathcal{DS}_j^\alpha}$. From a comparison of two trajectories

$$\begin{aligned} e^{t\Lambda^2} b &= [e^{t\lambda_0^2} b_0, ..., e^{t\lambda_{N\text{-}1}^2} b_{N\text{-}1}] \\ t^{tI} b &= [e^t b_0, ..., e^t b_{N\text{-}1}] \end{aligned}$$

for $t < 0$, we can observe that $\mathcal{DS}_0^\alpha$ is exponentially expanded from $\overline{\mathcal{DS}_0^\alpha}$ in all $i(= 1, ..., N\text{-}1)$-th axises, while $\mathcal{DS}_{N\text{-}1}^\alpha$ is shrunk from $\overline{\mathcal{DS}_{N\text{-}1}^\alpha}$ in all $i(= 0, ..., N-2)$-th axises. $\mathcal{DS}_i^\alpha$ is exponentially expanded from $\overline{\mathcal{DS}_i^\alpha}$ in all $k(> i)$-th axises and shrunk in all $k(< i)$-th axises (Figure 7).

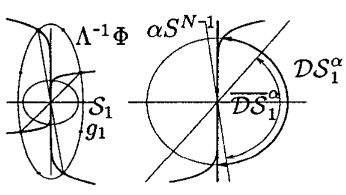

a) ROC b)

Figure 7 Comparison between $\Lambda^{\text{-}1}\mathcal{BR}_i$, $\overline{\mathcal{DS}_i^\alpha}$ and $\mathcal{DS}_i^\alpha$

Furthermore $||g_i|| : ||g_j|| = \lambda_i^{\text{-}1} : \lambda_j^{\text{-}1}$, i.e. $||g_i|| < ||g_j||$ if $\lambda_i > \lambda_j$. Therefore, we have

Theorem 2 (Regions of Convergence of FS-CMA) Let g_i be the local minima of FS-CMA for a $T/2$-spaced channel c and let C be the channel convolution matrix. Denote $\mathcal{S}(g_i)$ as the convergence region of g_i.

I. $\mathcal{S}(g_i)$ are exponential hyper-cones centered on g_i

II. Let $||g_0|| < ||g_1|| < \cdots < ||g_{N\text{-}1}||$, then for $\alpha < \lambda_0^{\text{-}1}$

$$\text{Vol}\,\mathcal{DS}_0^\alpha > \text{Vol}\,\mathcal{DS}_1^\alpha > \cdots > \text{Vol}\,DS_{N\text{-}1}^\alpha \quad (17)$$

as $\alpha \to 0$. And for $\alpha \gg \lambda_{N\text{-}1}^{\text{-}1}$

$$\text{Vol}\,\mathcal{DS}_0^\alpha < \text{Vol}\,\mathcal{DS}_1^\alpha < \cdots < \text{Vol}\,DS_{N\text{-}1}^\alpha \quad (18)$$

Notice that if we initialize CMA near the origin with single or double spike (i.e, $f = [0 \cdots 0\ 1\ (1)\ 0 \cdots 0]$), it is likely that the initailization lies in a region of convergence of a CM local minima with small noise gain by theorem 2.

5. CONCLUSION

We characterized the regions of convergence of FSE-CM corresponding to the different system delays. The regions of convergence are exponential hyper-cones. Near the origin, the CM solutions of small noise gain has an exponentially large region of convergence. This result suggests that a spike initialization with constrained magnitude would lie in the ROC of a small noise gain with a high probability. The implication of this result for noisy and undermodelled systems is yet to be studied.

6. REFERENCES

[1] W. M. Boothby, *An introduction to differentiable manifolds and Riemannian Geometry*, Academic Press, Inc., 1986.

[2] W. Chung, J. P. LeBlanc, "The local minima of fractionally-spaced CMA blind equalizer cost function in the presence of channel noise," *Proc. of IEEE Conf. Acoust., Speech, Signal Processing*, May 1998.

[3] I. Fijalkow, A. Touzni, and J. R. Treicher, "Fractionally spaced equalization using CMA: robustness to channel noise and lack of disparity," *IEEE transactions on Signal Processing*, vol. 45, no.1 pp. 55-66, Jan. 1997.

[4] C. R. Johnson, Jr., P. .B. Schniter, T. S. Endres, J. M. Behm, D. R. Brown, and R. A. Casas, "Blind Equalization Using the Constant Modulus Criterion: A Review," *Proc. IEEE*, 1998.

[5] J. P. Leblanc, C. R. Johnson, Jr., "Global CMA Error Surface Characteristics, Source Statistics Effects: Polytopes and Manifolds," 13^{th} *Int. Conf. on DSP*, (Santorini, Greece) Jul. 1997.

[6] H.H. Zeng, L. Tong and C. R. Johnson, Jr., "Relationships between the constant modulus and Wiener receivers," *IEEE Trans. Info. Theory*, 1998.